

## DEVELOPMENT OF DSSC PHOTOVOLTAIC CELLS FOR ENERGY PRODUCTION THROUGH THE RECOVERY OF WINEMAKING BY-PRODUCTS

Manuel Meneghetti<sup>1\*</sup>, Aldo Talon<sup>1</sup>, Elti Cattaruzza<sup>1</sup>, Emilio Celotti<sup>2</sup>, Elisabetta Bellantuono<sup>2</sup>, Enrique Rodríguez-Castellón<sup>3</sup>, Elisa Moretti<sup>1#</sup>

(1) Department of Molecular Sciences and Nanosystems, Ca'Foscari University of Venice, Via Torino 155/B, 30172 Venice – Italy.

(2) Department of Agricultural, Food, Environmental and Animal Sciences (DI4A), University of Udine, Via delle Scienze 208, 33100 Udine – Italy.

(3) Department of Inorganic Chemistry, Crystallography and Mineralogy, University of Málaga, Campus de Teatinos, E-29071 Málaga – Spain.

\*manuel.meneghetti@unive.it; #elisa.moretti@unive.it.

### Abstract

In this study a nanostructured titanium dioxide, with high surface area and ordered porosity, was prepared by sol-gel procedure and thermally treated at high temperature. Its structural, chemical and optical properties were studied by XRD, FEG-SEM, N<sub>2</sub> physisorption and DRS. Tannins and anthocyanins extracted from winemaking lees were then adsorbed on this porous support. After building a dye-sensitized solar cell (DSSC) prototype, several tests were carried out to evaluate the cell power and the photocurrent generated under simulated solar light irradiation. Using polyphenolic compounds as dyes in photovoltaic cells can represent an extremely eco-friendly and low environmental impact solution for electricity generation, transforming an agri-food waste into a resource and improving the environmental index of wineries.

### 1. Introduction

Global energy consumption is currently based on fossil fuels (oil, natural gas and coal) but, in recent years, due to the decreasing availability of non-renewable resources and the increasing energy demand, the scientific world has pushed the research on more sustainable and renewable resources<sup>1</sup>. In particular the solar energy, the best renewable and clean source of our planet, has been much more studied, optimizing materials, technologies and processes to obtain green electrical energy. Photovoltaic cells are devices able to convert solar energy directly into electricity by the photovoltaic effect. Even though these systems are unanimously considered very promising for clean energy production, their deployment is sometimes hindered by production costs, material availability and toxicity. Silicon-based systems (crystalline and amorphous) are a good compromise between costs and efficiency and have been much developed by photovoltaic industries during the last years, becoming the most diffused photovoltaic devices in the world. Despite this, technologies based on use the of organic compounds in photovoltaic cells are raising interest because they could be a viable alternative of conventional cells for their much lower environmental impact and low-cost production. In 1991 Graetzel and O'Regan introduced to the world a new type of photovoltaic devices: the DSSCs, acronym of Dye Sensitized Solar Cells, a system based on nanocrystalline TiO<sub>2</sub> and organic dyes. Since their breakthrough, DSSCs have attracted interest from all the academic and industrial community, that tried to improve their efficiency, reducing at the same time productions costs. Unlike silicon solar cells, DSSC charge generation and transport does not happen in a single material but is split in different layers: appropriate band gap semiconductor, sensitized dye and iodine-based electrolyte. In general, the device can be associated with a sandwich-type structure in which each layer has to respect specific chemical-physical requirements as has specific and well-defined functions in the electric current generation process. It is composed of (from the bottom): a counter-electrode, an electrolyte solution to close the circuit, a sensitizing dye, a nanostructured semiconductor, generally a non-toxic oxide, and finally, a conductive glass (Figure

1). One of the most important cells' elements is the dye, which can absorb sunlight moving electrons to a higher energy level, called excited state. Charge separation occurs at dye-semiconductor interface: electrons are injected into titanium dioxide layer and oxidized dye holds the positive charge. When the circuit is closed, electrons can travel through the semiconductor, transparent conductive electrode, external circuit, react with electrolyte and reach the positive charge, bringing back the dye molecules to fundamental state.

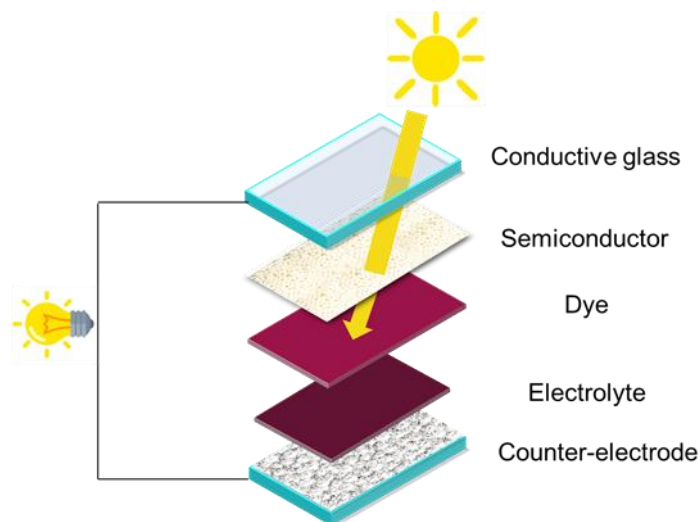


Figure 1. Schematic DSSC composition, under sunlight radiation.

This kind of solar cells is environmentally friendly and emulates the chlorophyll photosynthesis process which takes place inside leaves, where photons are absorbed by chlorophylls, explaining the fundamental role of the dyes in DSSCs. On the other hand, also the semiconductor layer is very important in the electron conduction and transport processes in a photovoltaic cell, and chemical-physical properties can influence the final efficiency of the device. A suitable semiconductor has to display a wide band gap that can fit the HOMO-LUMO dye energy level, a nanostructured morphology, relatively high surface area, pore volume and diameter for a proper dye adsorption and large crystallite domains to decrease traps-level recombination of carriers. For these reasons, an appropriate semiconductor for dye sensitized solar cells is titanium dioxide,  $\text{TiO}_2$ , that shows a band gap of 3.0-3.2 eV, can be prepared as a nanostructured material, with tunable surface area and pore size distribution.

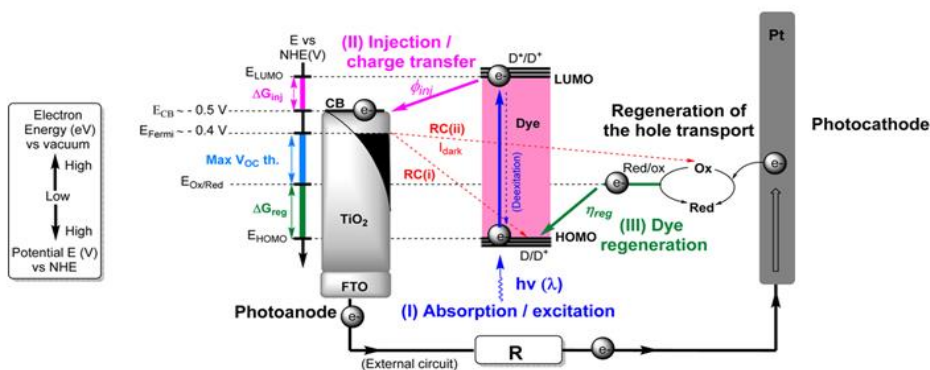


Figure 2. Schematic energy levels diagram of a DSSC <sup>2</sup>.

Titania structure can be influenced by different deposition techniques. The most used approaches to prepare this semiconductor film, characterized by a good electrical conductivity, high surface area and porosity, are tape casting and screen printing<sup>3-4-5</sup>. In both cases, a paste made up of titania

dispersed in suitable solvents and additives to obtain a colloidal system is used. Selected dye molecules, able to generate electrons under solar illumination, are then adsorbed on this thin layer. Metallorganic dyes, based on ruthenium and osmium polypyridyl complexes, have been widely employed as efficient sensitizers<sup>6-7</sup>. Unfortunately, this kind of metal complexes is usually obtained with multistep reactions and expensive chromatographic purification procedures<sup>1</sup>. An alternative to the use of transition metals can lead to a significant reduction of manufacturing costs of the final device<sup>8-9-10</sup>. Several natural dyes such as anthocyanin<sup>11-12</sup>, tannin<sup>13</sup>, carotenoid<sup>14-15</sup>, flavonoid<sup>8-16</sup> and chlorophyll<sup>17-18</sup> have also been used as sensitizer in DSSC<sup>1-8</sup> exhibiting high conversion efficiency. These are natural pigments contained in fruits and vegetables and are completely biodegradable, eco-friendly, easily available and with good light absorbance.

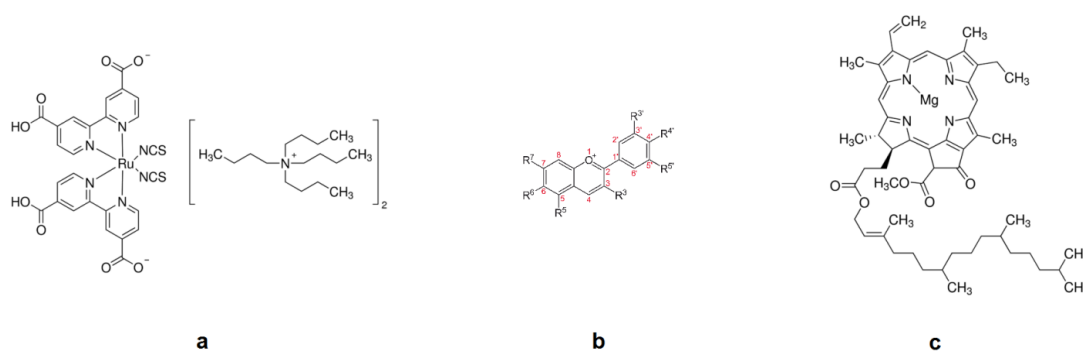


Figure 3. Three molecules commonly used in DSSC devices. From left: a) ruthenium complex N719, b) anthocyanin and c) chlorophyll-a.

All these molecules can be extracted, among others, from blueberries, oranges, eggplants, blackberries, currants, raspberries, olives and naturally grapes<sup>19</sup>. Nevertheless, an ethical question arises, since food has to be used and destroyed to obtain dyes from fruits and vegetables. Therefore, developing such a technology on a large scale could be considered incorrect from an ethical point of view and, at the end, economically disadvantageous too. It is necessary to recover and exploit the concept of circular economy, which considers the whole product's life-cycle, from its production to the creation of markets for waste-derived raw materials.

Waste-to-energy is a broad term that encompasses various waste treatment processes generating energy (e.g. in the form of electricity, heat or produce a waste-derived fuel), each of which has different environmental impacts and circular economy potential.

The innovative idea behind this applied research work, developed in collaboration with the University of Udine, the University of Málaga and a venetian winery located in the Prosecco region, consists in recovering and valorizing, through innovative solutions, the waste of winemaking process called "lees", for the realization of DSSC solar cells. Generally, at the end of winemaking and clarification wine process, the precipitate that remains on the bottom are the so-called dregs, composed of many organic materials and a large amount of bentonite, a natural phyllosilicate clay used by wineries to reduce protein instability and precipitate suspended solids responsible for wine turbidity<sup>20</sup>. Moreover, bentonite slightly bleaches white and red wines absorbing molecules responsible of wines color such as anthocyanins, tannins, catechins and polyphenols which, if properly extracted, can be valorized and used as dyes in DSSCs.

The current work aims to study a method to recover the main waste product of a winery, extracting the organic dyes contained in the lees, reintroducing them into the production cycle and transforming them into a resource to produce renewable and sustainable electricity from photovoltaic solar cells.

## 2. Experimental

## 2.1 Synthesis of nanostructure porous titania

Titanium dioxide powder was synthesized starting from a solution of titanium isopropoxide [ $\text{Ti}(\text{OC}_3\text{H}_7)_4$ ] (TTIP), acetic acid and polyethylene glycol phenyl ether in ethanol. Deionized water was added at room temperature under vigorous magnetic stirring in a TTIP: $\text{H}_2\text{O}$  molar ratio between 1.0:0.5 to 1.0:5.0. The white slurry product was left to age overnight to complete the sol-gel reaction (Figure 4).



Figure 4. Progress of sol-gel reaction to obtain white slurry  $\text{TiO}_2$  product.

Then the suspension was heated until the solvent was completely eliminated, replaced with water and transferred to an autoclave for hydrothermal treatment at 120-220 °C at autogenous pressure overnight. After this, the suspension was centrifuged and washed with deionized water and ethanol and finally dried in an oven.

## 2.2 Extraction of dyes from winemaking lees

Winemaking lees were collected in the first period of this year, 2019, from a venetian winery, partner of this research and situated in the Prosecco region (Conegliano, Italy). A suitable amount of lees was centrifuged at 6000 rpm, the solid was recovered and the same amount (w/w) of solvent (methanol, ethanol and mixtures of them), acidified with 1% v/v with concentrated HCl (37%), was added. The extraction process was monitored by evaluating the maximum of absorbance variation with an UV-Vis spectrophotometer. After 24 hours of extraction reaction, the dye solution was stored at 5 °C.

## 2.3 Realization of a dye-sensitized solar cell

A conductive glass like fluorine doped tin oxide (FTO) or indium doped tin oxide (ITO), used as photoanode, was cleaned in a detergent solution using an ultrasonic bath and then rinsed with water and ethanol. The cleaned working electrode was coated with a "blocking layer", a thin compact layer necessary to reduce leakage currents and enhance the performance of the device, and usually made by spray pyrolysis or spin coating techniques using a titanium precursor. In this study the deposition was performed by home-made spray pyrolysis technique, using an alcoholic solution of titanium diisopropoxide bis(acetylacetonate) on a heated substrate at 400 °C, to evaporate the solvent and obtain a compact layer of titanium dioxide.

The electrodes coated with  $\text{TiO}_2$  blocking layer were heated in air from room temperature to 350-600 °C for 30 minutes, to sinter this compact layer. On this, a layer of nanostructured porous titania with a thickness lower than 30  $\mu\text{m}$  was printed, using a viscous paste based on titanium dioxide powder dispersed with a terpenic dispersing agent in alcoholic solution. After the deposition of a porous titanium dioxide layer and its sintering, the plate was immersed in the natural dye solution in a dark container overnight to complete the sensitizer uptake. After soaking the film in this solution, dye molecules were left to be adsorbed on the surface of the titania. Dye-titania electrode acts like a photoanode, but to obtain electric current is necessary a counter-electrode, which provides to

catalyze the redox reaction of electrolyte that then reduce oxidized dye to fundamental state. A counter-electrode was prepared by thermal decomposition of an alcoholic  $H_2PtCl_6$  solution on a cleaned conductive transparent glass heated at 250 °C through spray pyrolysis technique. Dye-titania electrode and counter-electrode were finally assembled into a sandwich-type cell and sealed with a gasket made by a hot-melt resin. Some drops of an iodine-based electrolyte solution were introduced into the cell via vacuum backfill. The cell was put in a vacuum chamber and then, when atmospheric pressure was replaced, the electrolyte was pushed inside internal free space by pressure variation. After this step, the dye sensitized solar cell prototype was tested for photocurrent measurements.

## 2.4 Characterization techniques

The textural properties of titanium dioxide were characterized by nitrogen physisorption at -196°C with an ASAP 2010 Micrometrics sorptometer. The samples (about 0.1 g) were outgassed first at 130 °C for 12 h at 0.67 Pa and then at room temperature for 2 h at  $1 \times 10^{-4}$  Pa. To determine the specific surface areas the BET equation (S.A. BET) was applied and the specific pore volume ( $V_s$ ) was calculated at  $P/P_0 = 0.98$ . The pore size distribution was calculated according to the BJH method.

X-Ray diffraction (XRD) was used to determine the crystalline phases of titania, by using a Philips X'Pert system (Bragg-Brentano parafocusing geometry) with a nickel-filtered  $Cu K\alpha_1$  radiation at 0,154 nm. The samples were disc shaped pressed powders and profiles were collected before and after calcination. The average anatase and rutile crystallite size was determined on XRD peak broadening by the Scherrer equation (line width of the anatase (101) reflection at  $2\theta = 25.3^\circ$  and rutile (110) reflection at  $2\theta = 27.4^\circ$ ):

$$\tau = \frac{K \lambda}{\beta \cos \theta}$$

Where  $\tau$  is the crystallite size,  $K$  the shape factor,  $\lambda$  is the X-ray wavelength for  $Cu K\alpha_1$  radiation,  $\beta$  is the line broadening at FWHM and  $\theta$  is the Bragg angle.

To obtain the anatase:rutile weight fraction in the samples was used the following equation<sup>25</sup>:

$$Anatase (\%) = \frac{100}{\left(1 + 1,265 \frac{I_R}{I_A}\right)}$$

where  $I_A$  and  $I_R$  are the peak intensities of the (101) and (110) reflections for anatase and rutile, respectively.

Size and morphology of the nanoparticles were studied by Field Emission Gun Scanning Electron Microscopy (FEG-SEM) Zeiss with cutting-edge electro-optical design.

The band gap of titania was determined by Diffuse Reflectance UV-Vis Spectroscopy (DRS). Spectra were collected with a Perkin Lambda 35 UV-Vis spectrophotometer. The absorption coefficient ( $\alpha$ ) was calculated as follows:

$$\alpha = \frac{\ln \frac{1}{T}}{d}$$

where  $T$  is the measured transmittance and  $d$  is the optical path length.

Band gap energy,  $E_g$ , was determined thoroughly the  $\alpha$  value ( $m^{-1}$ ) from a plot of  $(\alpha h\nu)^{\frac{1}{2}}$  versus photon energy ( $h\nu$ ), where  $h$  is the Planck's constant and  $\nu$  is the frequency ( $s^{-1}$ ). The intercept of the tangent to the absorption curves was used to estimate the band gap ( $E_g$ ) value.

Dye extraction process was monitored by an Agilent 8453 UV-Vis spectrophotometer, following the absorbance at the maximum of UV-Vis spectrum, after water dilution. Dye solutions extracted with green solvents were characterized by various methods to determine concentrations of anthocyanins, catechins, tannins, polyphenols and intensity of color.

Anthocyanins extracted from winemaking lees were determined by the procedure of Ribereau Gayon and Stonestreet (1965)<sup>22</sup> with the bisulphite bleaching as anthocyanins form colorless compound with the bisulphite ion, thus transferring from the red colored flavylum cation to a non-colored form. Catechins were determined according to a method proposed by Zironi et al.<sup>23</sup>, using DAC (4-(dimethylamino)cinnamaldehyde). The assay was performed using a chromogen reagent of 1.0 g DAC dissolved in 250 mL of 37% HCl and 750 mL methanol. To 1 mL of 1:25 (v/v) diluted sample, 5 mL of DAC solution were added and, after 5 minutes, the maximum value of absorption at 640 nm was measured against a blank prepared by substituting sample with 1 mL of 10% ethanol.

Tannins characterization was carried out following the Weinges and Nader method<sup>24</sup>: an aliquot of 2 mL of sample diluted fifty times were added to a tube containing 6 mL of acidized butyl alcohol prepared by dissolving 150 mg Fe<sub>2</sub>(SO<sub>4</sub>) in 500 mL of 1-butanol and 500 mL of HCl 37%. Half of this solution was put in an oven at 100 °C for 30 minutes. After cooling, the optical density was measured at 550 nm for both solutions against water.

Polyphenols content of extracted dyes was evaluated using the Folin-Ciocalteu's method that involves the addition of 0.5 mL of Folin-Ciocalteu's reagent to 0.1 mL dye sample diluted 1:10 in water. After mixing, 2.0 mL of 15% Na<sub>2</sub>CO<sub>3</sub> were added and the volume was brought up to 10 mL with deionized water. The sample was kept in the dark for 2 hours and then absorbance was measured at 750 nm using as a blank a solution with deionized water instead of the dyes analyzed. The color intensity was determined as a sum of the absorbance at 420 nm, 520 nm and 620 nm following Glories method<sup>26</sup>, with an optical path of 10 mm.

The measurements of power ( $P$ ) and photocurrent ( $I$ ) generated by the obtained photovoltaic cell were performed by irradiating the prototype by a Sunlight Solar Simulator (AM 1.5G filter, 100 W Xenon arc lamp, Abet Technologies), to simulate the solar spectrum on earth surface, and using a digital multimeter (Tecktronix Keithley 2410) directly connected to the cell electrodes. The power against voltage  $P$ - $V$  curve was obtained by following equation:

$$P = V \cdot I$$

by the simultaneously measurements of flowing current,  $I$  and the cell voltage,  $V$ .

### 3. Result and discussion

The first part of this research work was focused on the characterization of the nanostructured porous titania, used in a photovoltaic DSSC cell as a semiconductor where organic dyes are adsorbed.

The morphology of the synthesized TiO<sub>2</sub> was evaluated by with FEG-SEM. It can be observed, in Figure 5, the presence of aggregated particles with a size lower than 100 nm, in the range of nanomaterials. As shown, the aggregation of the nanoparticles, as well as their size, increased by increasing the temperature, as expected for this type of oxide.

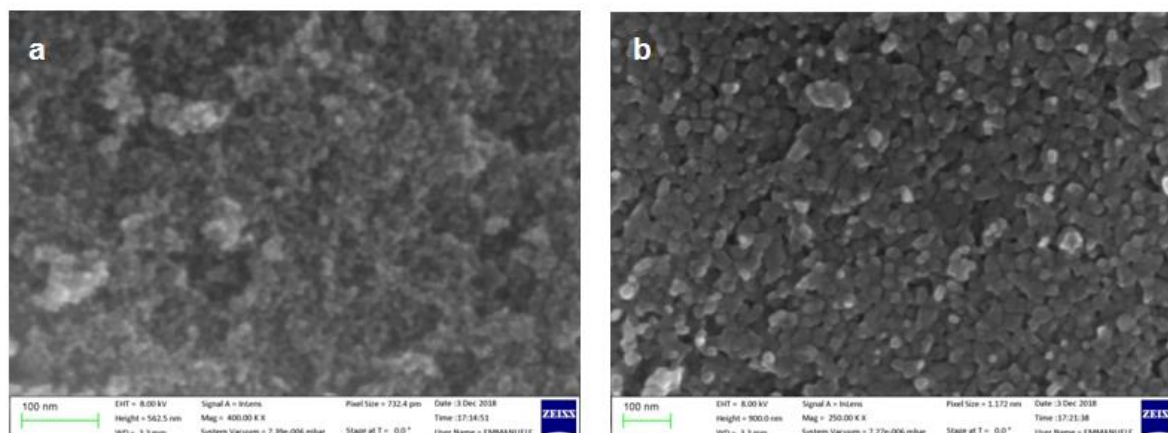


Figure 5. FEG-SEM micrograph of TiO<sub>2</sub> thermally treated at: a) 400°C and b) 600°C.

Nanostructured titania semiconductor was characterized by N<sub>2</sub> physisorption at -196 °C to evaluate the textural properties and the porosity formed during the sol-gel synthesis. The isotherms of all the prepared samples, both before (dried at 100°C) and after calcination (at 400°C and 600°C), are of type IV according to the IUPAC classification with a hysteresis loop, noticeable in Figure 6, indicating an ordered pore size distribution in the mesoporous region.

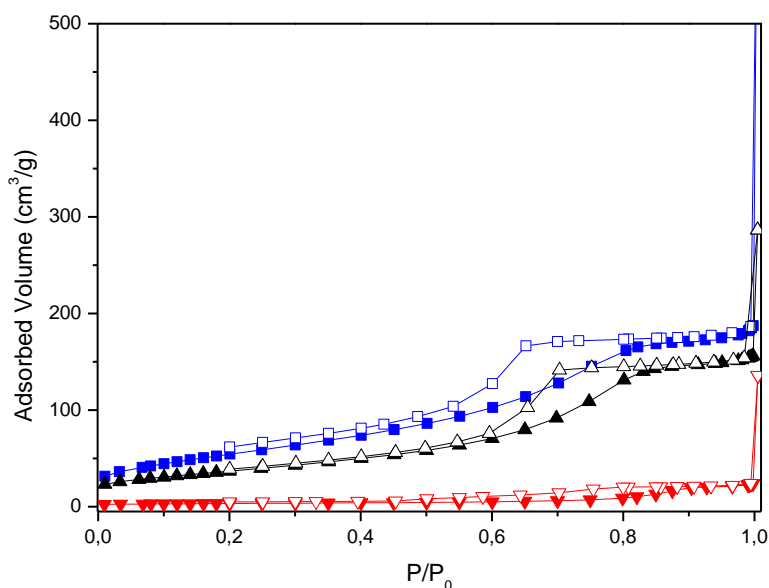


Figure 6. N<sub>2</sub> adsorption-desorption isotherms at -196°C of titania as synthesized (▼) and calcined at 400°C (■) and 600°C (▲). Filled symbols are referred to the adsorption branch and empty symbols to the desorption one.

Table 1 summarizes the most important structural properties of the prepared titania samples. Nanostructured titania sample, after synthesis, showed a very high specific surface area,  $SA_{BET}$ , of 205 m<sup>2</sup>g<sup>-1</sup>, a narrow pore diameter distribution lower than 20 nm and a pore volume of 0.28 cm<sup>3</sup>g<sup>-1</sup>. A correlation between the calcination temperature process and the textural features of these materials can be noticed. By increasing the calcination temperature, the surface area and pore volume of the semiconductor significantly decrease. This phenomenon, as already observed by FEG-SEM microscopy for the average size of the nanoparticles, is due to the reorganization of the crystalline structure that, thanks to thermal energy, move to a thermodynamically more stable structure.

Table 1. Textural parameter of titania semiconductor as a function of different thermal treatments.

T calcination (°C)	SA <sub>BET</sub> <sup>a</sup> (m <sup>2</sup> g <sup>-1</sup> )	V <sub>p</sub> <sup>b</sup> (cm <sup>3</sup> g <sup>-1</sup> )	A <sup>c</sup> (%)	R <sup>d</sup> (%)	Average Crystallite Size <sup>e</sup> (nm)
As-prepared sample	205	0.28	100	-	6.3 A
400	135	0.24	100	-	8.0 A
600	12	0.04	98	2	29.8 A 80.3 R

- a) Specific surface area obtained by the BET equation.  
 b) Cumulative pore volume calculated at  $p/p_0=0.98$ .  
 c) Anatase polymorph obtained by XRD.  
 d) Rutile polymorph obtained by XRD.  
 e) Determined by Scherrer equation.

Phase and crystallite size were determined by X-ray diffraction and Figure 7 shows the diffractograms of titania samples before and after calcination treatments. The diffraction peaks of the as-prepared and calcined at 400 °C samples can be indexed, in agreement with the values of standard cards, as typical anatase phase (JCPDS, PDF card no. 73–1764) of TiO<sub>2</sub>. When calcination temperature increases to 600 °C, the typical rutile (110) reflection becomes noticeable at  $2\theta = 27.4^\circ$  meaning the initial transformation of anatase phase into rutile polymorph. At the same time, the peaks are broad for the as-synthesized titania sample, meaning the formation of small crystallites during the particle growth in sol-gel synthesis process. When calcination temperature increases, an improved crystallinity is clearly noticeable. In fact, as a consequence of thermal treatment the intensity of anatase and rutile reflections becoming sharper and more intense, due to particles aggregation which leads to growth of larger crystal domains.

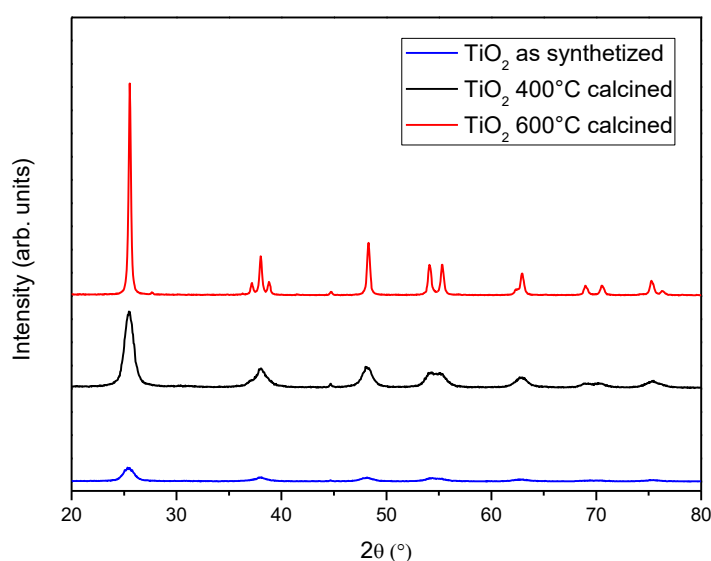


Figure 7. X-ray diffractograms of titania semiconductor samples thermally treated at different temperatures.

As expected, the calculated average size of anatase crystallites estimated from the FWHM of anatase (101) reflection at  $2\theta = 25.3^\circ$  and rutile (110) reflection at  $2\theta = 27.4^\circ$ , shows an increasing trend with the thermal treatment, from 6.3 nm for the as-prepared sample to 29.8 nm for the titania calcined at the highest used temperature (600 °C). The values of anatase and rutile weight fractions, reported in Table 1 and determined by the method described in experimental section, shows the presence of only anatase in as synthesized and 400 °C calcined titania. Transformation from anatase to rutile phase is visible at 600 °C. This means that a phase transformation occurs at elevated temperature.

Dye Sensitized Solar Cells efficiency is influenced by many factors, among which the most important are the semiconductor's properties. An increasing crystallite domain, due to high calcination temperature, usually leads to a decrease in traps-level number, thus increasing the final electrical current. On the other hand, a thermal treatment at high temperature reduces the surface area and pore volume of the nanostructured titania, decreasing the available area for dye absorption. For these reasons, this peculiar titania thermally treated at 600 °C was discarded for the realization of a photovoltaic cell, trying to reach a suitable compromise between high surface area, pore volume, pore diameter and good crystallinity to improve electrical current.

Another important characterization consists in evaluate the photo-responsive behavior of titanium dioxide, because usually it absorbs only a small fraction of solar radiations, precisely in UV-region. This behavior is due to band gap, the difference between conductive and valence band, that is situated around 3,0 eV for rutile phase and 3,2 eV for anatase phase and can influence the energy level involved in electrons transfer process of dye sensitized solar cells, as reported in Figure 2.

The titania sample calcined at 400 °C was characterized by Diffuse Reflectance UV-Vis Spectroscopy (DRS) to determine its band gap value. An absorption peak in the UV region (below 400 nm), due to intrinsic absorption of titanium dioxide, was recorded (Figure 8).

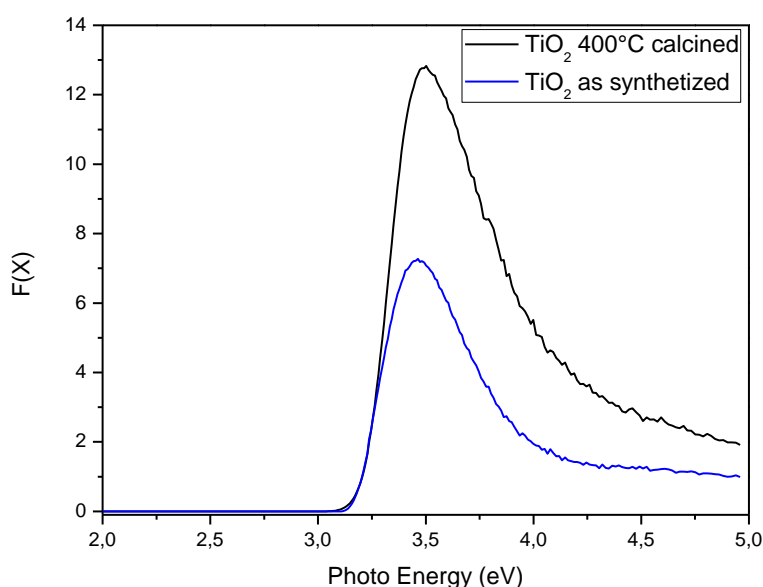


Figure 8. DRS spectra of fresh and calcined (400°C) titanium dioxide.

As expected for this type of semiconductor materials, the band gap of titanium dioxide samples, both as-prepared and calcined, was about the theoretical value of 3.2 eV that confirming the large content of anatase phase.

In this study, dye extraction process starts from winemaking lees of Merlot-Cabernet wines, composed of many organic materials and a large amount of bentonite. Bentonite absorbs molecules responsible of wines color, such as anthocyanins, tannins, catechins and polyphenols, that with the proper extraction process can be reused as sensitizers. After centrifugation of winemaking lees, in order to separate the solid from the supernatant, a semi-solid colored material (Figure 9) was used to extract a dye solution, needed for the construction of a DSSC photovoltaic cell.



Figure 9. Semi-solid winemaking lees.

From UV-Vis spectrum of the diluted dye sample extract, a large absorption band centered at 525 nm can be noticed (Figure 10a). This maximum was used to monitor the concentration of dye solution during the extraction process, as a function of extraction time.

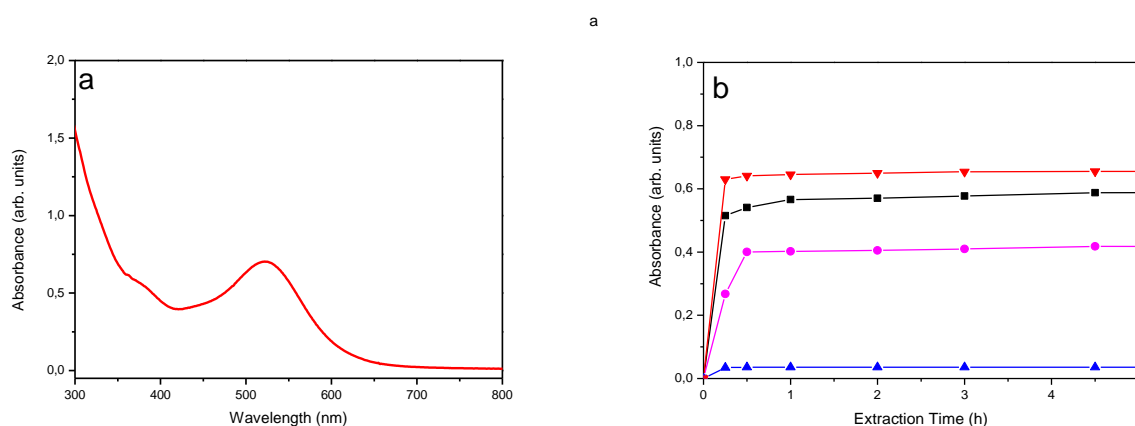


Figure 10. a) UV-Vis spectrum of extracted dye in water; b) absorbance vs extraction time.

The kinetics of the dye extraction process, shown in Figure 10b, proves that dye extraction from bentonite occurs in some hours. For all solvents used, absorbance increases rapidly in the first hour, and then increases very slowly with an asymptotic behavior. We can suppose that, at the beginning of the extraction process, solvent desorbs dye molecules from the external structure of bentonite layers and then extract organic molecules located in the middle of the clay layers.

After optimizing the extraction process, the organic molecules were further characterized, or the concentration of the different molecules involved in color appearance evaluated. Anthocyanins, tannins, catechins, and total polyphenols concentrations are reported in Figure 11.

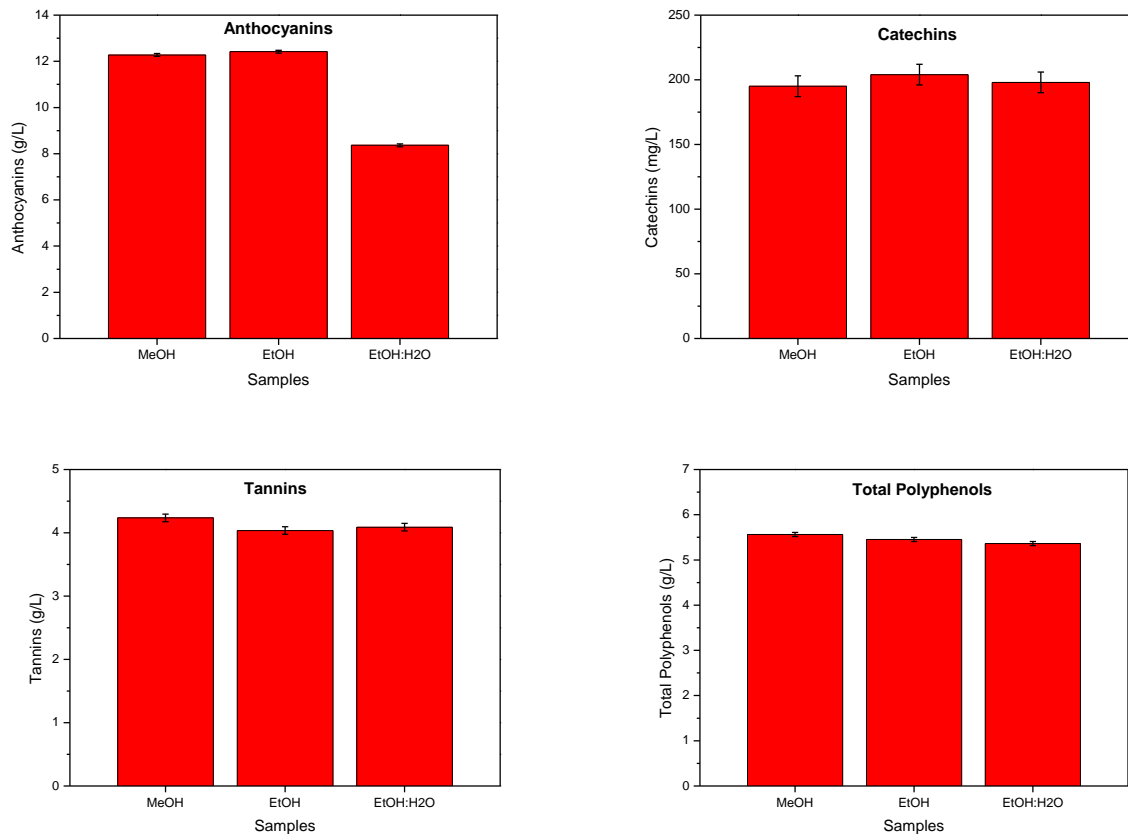


Figure 11. Anthocyanins, tannins, catechins, and total polyphenols characterizations of extracted dye.

In particular, the anthocyanins responsible for red color are very concentrated (10 g/L), compared to typical values of anthocyanins content in red wine, like 109 mg/L for Merlot and 125 mg/L for Cabernet wine<sup>21</sup>. The presence of water is responsible of the decreasing of dye concentration in the extract, probably due to the different solubility of these molecules in organic and aqueous solutions. Another important characterization, reported in Figure 12, is the color intensity that was determined as the sum of the absorbance values at 420 nm, 520 nm and 620 nm.

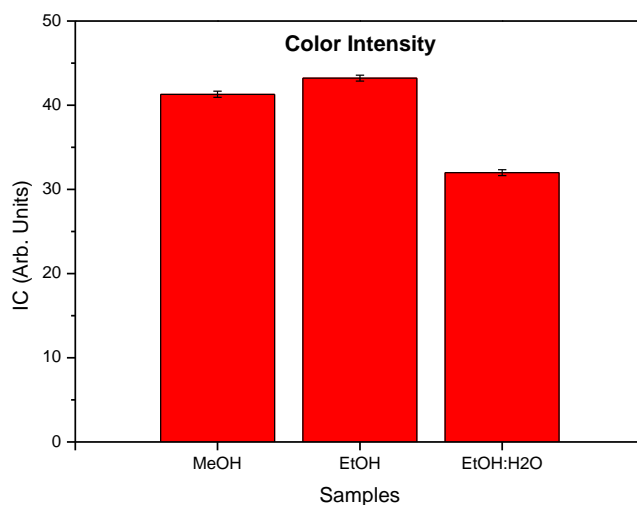


Figure 12. Color intensity of extracted dyes with methanol, ethanol and a water/ethanol mixture.

Color intensity, independently by the type of dye molecules, can indicate the presence of low or high dyes concentration that is a necessary condition to absorb high amount of dye on the semiconductor layer. After impregnation, the cell was assembled, and photocurrent tests were performed to evaluate the cell power and the photocurrent generated in the presence of a solar (Figure 13).



Figure 13. A Dye Sensitized Solar Cells prototype, assembled by valorizing winemaking waste, tested under simulated solar light irradiation.

The recorded I-V and P-V curves, shown in Figure 14, can be used to determine the characteristic proprieties of a photovoltaic solar cell. The performance of a natural DSSC is usually evaluated by measuring the open circuit voltage ( $V_{OC}$ ) and the short circuit current density ( $J_{SC}$ ). For this cell prototype, the measured open circuit voltage was 0.42 V, the short circuit current 1.1 mA/cm<sup>2</sup> and the power density 0.25 mW/cm<sup>2</sup>, comparable with the typical values of an organic dye sensitized solar cell<sup>19</sup>.

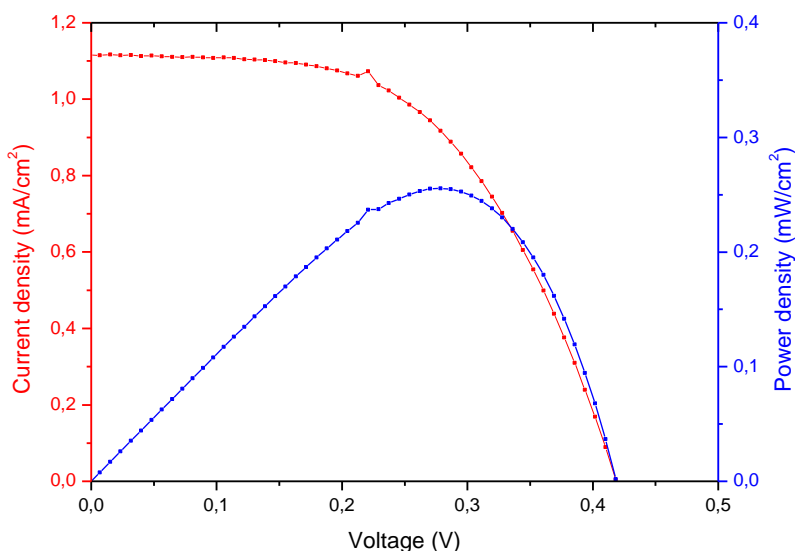


Figure 14. I-V and P-V curves of the DSSC prototype realized with a winemaking lees extract.

#### 4. Conclusions

The present work aimed to exploit and valorise, through innovative solutions, the main waste product of the wineries, recovering the lees of red and white wines to realize DSSC solar cells and generate renewable and sustainable photoelectric current. A nanostructured mesoporous titanium dioxide was synthesized by a sol-gel process, thermally treated at different temperatures and characterized by several techniques. Organic dyes (tannins, anthocyanins, polyphenols, catechins), after extraction from winemaking lees and characterization with typical wine analyses to estimate the concentrations of each dye and the color intensity, were adsorbed on this high surface area oxidic matrix. A DSSC prototype was then assembled and tested under simulated solar light irradiation and the generated electrical current was measured. This innovative solar cell can be considered a molecular machine that works in the nanotechnology field and can be seen as a sustainable and low-cost alternative to traditional systems based on silicon, transforming an agri-food waste in resource to produce electrical green energy.

#### Acknowledgments

The authors would like to acknowledge Dr. Giorgio Serena, Dr. Luca Serena, Dr. Stefano Meneghetti and Dr. Antonio Barzan of Azienda Vinicola Serena (Conegliano, Italy) for the valuable and constructive suggestions during the planning and development of this research work.

M.M. thanks Veneto Region and European Social Found (FSE) operational programme (OP) for financial support of 2120-1-11-2018 Project.

#### References

- 1) G. Calogero, A. Bartolotta, G. Di Marco, A. Di Carlo, F. Bonaccorso, Vegetable-based dye sensitized solar cells, *Chem. Soc. Rev.* 44 (2015) 3244-3294.
- 2) Y. Duan, J. Zheng, M. Xu, X. Song, N. Fu, Y. Fang, X. Zhou, Y. Lin, Metal and F dual-doping to synchronously improve electron transport rate and lifetime for TiO<sub>2</sub> photoanode to enhance dye-sensitized solar cells performances, *J. Mater. Chem. A* 3 (2015) 5692.
- 3) J. Gong, J. Liang, K. Sumathy, Review on dye-sensitized solar cells (DSSCs): Fundamental concepts and novel materials, *Renew. Sustainable Energy Rev.* 16 (2012) 5848-5860.
- 4) P. Gemeiner, M. Mikula, Efficiency of dye sensitized solar cells with various compositions of TiO<sub>2</sub> based screen printed photoactive electrodes, *Acta Chem. Slov.* 6 (2013) 29-34.
- 5) K.E. Lee, C. Charbonneau, G.P. Demopoulos, Thin single screen-printed bifunctional titania layer photoanodes for high performing DSSCs via a novel hybrid paste formulation and process, *J. Mater. Res.* 28 (2013) 480-487.
- 6) R. Argazzi, G. Larramona, C. Contado, C.A. Bignozzi, Preparation and photoelectrochemical characterization of a red sensitive osmium complex containing 4,4',4''-tricarboxy-2,2':6',2''-terpyridine and cyanide ligands, *J. Photochem. Photobiol. A* 164 (2004) 15-21.
- 7) M.K. Nazeeruddin, P. Péchy, T. Renouard, S.M. Zakeeruddin, R. Humphry-Baker, P. Comte, P. Liska, L. Cevey, E. Costa, V. Shklover, L. Spiccia, G.B. Deacon, C.A. Bignozzi, M. Grätzel, Engineering of efficient panchromatic sensitizers for nanocrystalline TiO<sub>2</sub>-based solar cells, *J. Am. Chem. Soc.* 123 (2001) 1613-1624.
- 8) N.A. Ludin, A.M. Al-Alwani Mahmoud, A. Bakar Mohamad, A.H. Kadhum, K. Sopian, N.S. Abdul Karim, Review on the development of natural dye photosensitizer for dye-sensitized solar cells, *Renew. Sustainable Energy Rev.* 31 (2014) 386-396.

- 9) M.R. Narayan, Review: dye sensitized solar cells based on natural photosensitizers, *Renew. Sustainable Energy Rev.* 16 (2012) 208-212.
- 10) K. Wongcharee, V. Meeyoo, S. Chavadej, Dye sensitized solar cell using natural dyes extracted from rosella and blue pea flowers, *Sol. Energy Mater. Sol. Cells* 91 (2007) 566.
- 11) N.J. Cherepy, G.P. Smestad, M. Grätzel, J.Z. Zhang, Ultrafast electron injection: implications for a photoelectrochemical cell utilizing an anthocyanin dye sensitized TiO<sub>2</sub> nanocrystalline electrode *J. Phys. Chem.* 101 (2007) 9342-9351.
- 12) H. Chang, Y.J. Lo, Pomegranate leaves and mulberry fruit as natural sensitizers for dye-sensitized solar cells *Sol. Energy* 84 (2010) 1833-1837.
- 13) M. Kamel, R.M. El-Shishtawy, B.M. Youssef, H. Mashaly, Ultrasonic assisted dyeing: III. Dyeing of wool with lac as a natural dye, *Dyes Pigm.* 65 (2005) 103-110.
- 14) S. Kishimoto, T. Maoka, K. Sumitomo, A. Ohmiya, Analysis of carotenoid composition in petals of *Calendula* (*Calendula officinalis* L), *Biosci. Biotechnol. Biochem.* 69 (2005) 2122-2128.
- 15) N.M. Gomez-Ortiz, I.A. Vazquez-Maldonado, A.R. Perez-Espadas, G.J. Mena-Rejon, J.A. Azamar-Barrios, G. Oskam, Dye-sensitized solar cells with natural dyes extracted from achiote seeds, *Sol. Energy Mater. Sol. Cells* 94 (2010) 40-44.
- 16) K. Davies, *Plant Pigments and Their Manipulation*, Annual Plant Reviews vol 12 (2004).
- 17) Y. Amao, Y. Yamada, Photovoltaic conversion using Zn chlorophyll derivative assembled in hydrophobic domain onto nanocrystalline TiO<sub>2</sub> electrode, *Biosens. Bioelectron.* 22 (2007) 1561-1565.
- 18) X-F Wang, H. Tamiaki, L. Wang, N. Tamai, O. Kitao, H. Zhou, S-I. Sasaki, Chlorophyll-a derivatives with various hydrocarbon ester groups for efficient dye-sensitized solar cells: static and ultrafast evaluations on electron injection and charge collection processes *Langmuir* 26 (2010) 6320-6327.
- 19) G. Calogero, J-H Yum, A. Sinopoli, G. Di Marco, M. Gratzel, M. Khaja Nazeeruddin, Anthocyanins and betalains as light-harvesting pigments for dye sensitized solar cells, *Solar Energy* 86 (2012) 1563-1575.
- 20) E. Lira, F.N. Salazar, J.J. Rodriguez-Bencomo, S. Vincenzi, A. Curioni, F. Lopez, Effect of using bentonite during fermentation on protein stabilization and sensory properties of white wine, *Int. J. of Food Science and Technology*, 49 (2014) 1070-1078.
- 21) M. A. Cliff, M. C. King, J. Schlosser, Anthocyanin, phenolic composition, colour measurement and sensory analysis of BC commercial red wines, *Food Research International* 40 (2007) 92-100.
- 22) P. Ribereau-Gayon, E. Stonestreet, *Bull. Soc. Chim.*, 9 (1965) 2649-2652.
- 23) R. Zironi, S. Buiatti, E. Celotti, Evaluation of a new colourimetric method for the determination of catechins in musts and wines, *Vitic. Enol. Sci.* 47 (1992) 1-7.
- 24) K. Weinges, F.W. Nader, Proanthocyanidns. In *Anthocyanins as food colors*, Academic Press - New York (1982) 93-120.
- 25) D. Mardare, M. Tasca, M. Delibas, G.I. Rusu, On the structural properties and optical transmittance of TiO<sub>2</sub> r. f. sputtered thin films, *Appl. Surface Sci.* 156 (2000) 200-206.
- 26) Y. Glories, *La coluler des vins rouges. Mesure, origine et interpretation. Connais. Vigne Vin*, 18 (1984) 253-271.